

CATR: Combinatorial-Dependence Audio-Queried Transformer for Audio-Visual Video Segmentation

Kexin Li
Zhejiang University
Hangzhou, China
12221004@zju.edu.cn

Zongxin Yang*
Zhejiang University
Hangzhou, China
yangzongxin@zju.edu.cn

Lei Chen
Finvolution Group
Shanghai, China
chenlei04@xinye.com

Yi Yang
Zhejiang University
Hangzhou, China
yangyics@zju.edu.cn

Jun Xiao
Zhejiang University
Hangzhou, China
junx@cs.zju.edu.cn

ABSTRACT

Audio-visual video segmentation (AVVS) aims to generate pixel-level maps of sound-producing objects within image frames and ensure the maps faithfully adhere to the given audio, such as identifying and segmenting a singing person in a video. However, existing methods exhibit two limitations: 1) they address video temporal features and audio-visual interactive features separately, disregarding the inherent spatial-temporal dependence of combined audio and video, and 2) they inadequately introduce audio constraints and object-level information during the decoding stage, resulting in segmentation outcomes that fail to comply with audio directives. To tackle these issues, we propose a decoupled audio-video transformer that combines audio and video features from their respective temporal and spatial dimensions, capturing their combined dependence. To optimize memory consumption, we design a block, which, when stacked, enables capturing audio-visual fine-grained combinatorial dependence in a memory-efficient manner. Additionally, we introduce audio-constrained queries during the decoding phase. These queries contain rich object-level information, ensuring the decoded mask adheres to the sounds. Experimental results confirm our approach's effectiveness, with our framework achieving a new SOTA performance on all three datasets using two backbones. The code is available at <https://github.com/aspirinone/CATR.github.io>.

CCS CONCEPTS

• Computing methodologies → Video segmentation.

KEYWORDS

Combinatorial-Dependence; Audio-Constrained Queries; Blockwise-Encoded Gate

*Zongxin Yang is the corresponding author.

Permission to make digital or hard copies of all or part of this work for personal or classroom use is granted without fee provided that copies are not made or distributed for profit or commercial advantage and that copies bear this notice and the full citation on the first page. Copyrights for components of this work owned by others than the author(s) must be honored. Abstracting with credit is permitted. To copy otherwise, or republish, to post on servers or to redistribute to lists, requires prior specific permission and/or a fee. Request permissions from permissions@acm.org.

MM '23, October 29–November 3, 2023, Ottawa, ON, Canada.

© 2023 Copyright held by the owner/author(s). Publication rights licensed to ACM.
ACM ISBN 979-8-4007-0108-5/23/10...\$15.00
<https://doi.org/10.1145/3581783.3611724>

ACM Reference Format:

Kexin Li, Zongxin Yang, Lei Chen, Yi Yang, and Jun Xiao. 2023. CATR: Combinatorial-Dependence Audio-Queried Transformer for Audio-Visual Video Segmentation. In *Proceedings of the 31st ACM International Conference on Multimedia (MM '23)*, October 29–November 3, 2023, Ottawa, ON, Canada. ACM, Ottawa, Ontario, Canada, 10 pages. <https://doi.org/10.1145/3581783.3611724>

1 INTRODUCTION

Audio-visual video segmentation (AVVS) aims to generate pixel-level maps of sound-producing objects within image frames and ensure the maps faithfully adhere to the given audio. For instance, when a person sings, AVVS enables the identification and segmentation of individuals in the video (see Figure 1 (a)). This capability has significant implications for various applications, such as video editing and surveillance. Despite the successful integration of multi-modal guidance approaches using point, box, scribble, text, and verbal cues for segmentation in recent studies [6, 14, 58], audio guidance has not yet been incorporated. This gap can be attributed to the inherent challenges of AVVS, including the ambiguous semantic information embedded in sounds and establishing correspondence between sounds and pixel-level predictions. Therefore, future research needs to investigate the integration of multi-knowledge representations [46], including audio, video, segmentation, etc.

In the domain of referring video object segmentation [18, 40, 58] and audio-visual understanding [8, 21, 21–23, 31, 34, 35, 41–44, 50, 56], substantial efforts have been devoted to investigating multi-modal segmentation techniques. Zhou et al. [55], for example, introduced a framework incorporating the TPAVI module, which facilitates audio-visual pixel-level segmentation. However, these methods still encounter two primary limitations in the realms of audio fusion and audio-guided video decoding:

Firstly, **Separate-Dependence Fusion**. The challenges in utilizing audio features arise from the ambiguous semantic information embedded within sounds, such as differentiating a child's cry from a cat's meow, in contrast to the clear linguistic references to "child" and "cat". As a result, establishing precise pixel-level associations under these indeterminate auditory cues is difficult. However, we found that audio has a unique advantage: its temporal properties align with those of video features, capturing distinct but complementary aspects of the same event. Existing methods do not fully exploit this property, addressing video temporal information and

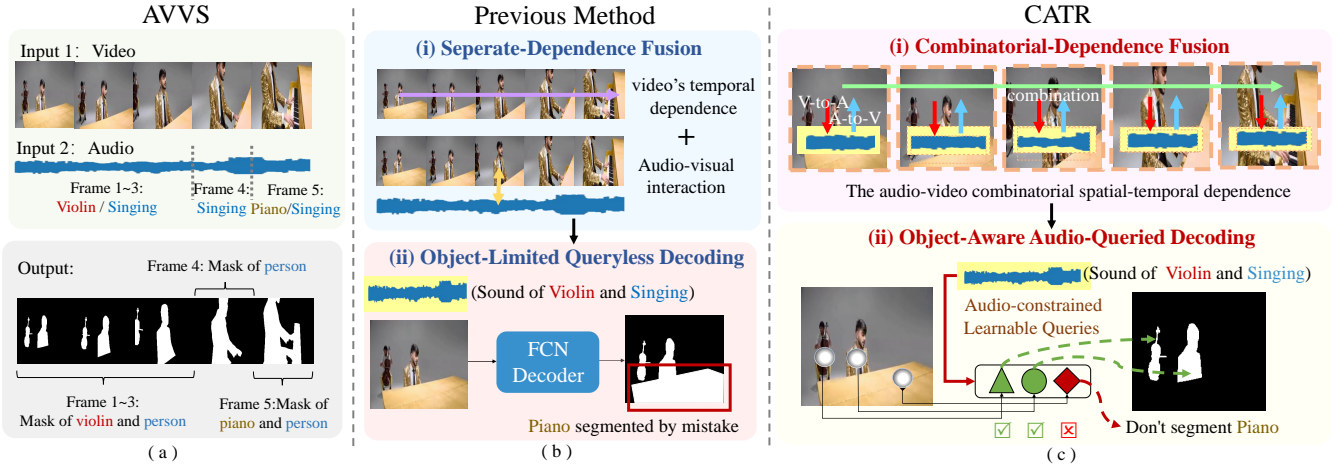


Figure 1: AVVS Task Description and CATR Contributions. The objective of the Audio-Visual Video Segmentation (AVVS) task is to generate pixel-level maps identifying sound-producing objects within image frames (a). Previous approaches separately addressed the temporal dependencies of video and the audio-video interaction information (b), neglecting the unique spatial-temporal dependencies inherent to audio and video as a combination. CATR initially merges audio and video features, subsequently capturing the spatial-temporal dependencies of this combination. Note that the red arrow symbolizes the Video-to-Audio (V-to-A) information, while the blue arrow denotes the Audio-to-Video (A-to-V) information. Additionally, we introduce innovative audio-constrained learnable queries to enhance object-aware segmentation (c).

audio-visual interactions separately, which constrains their effectiveness. Various combinations of audio and video exhibit unique spatial-temporal dependencies, contributing to more accurate and robust results. Thus, a method that captures the spatial-temporal characteristics of audio and video in combination is essential.

Secondly, **Object-Limited Queryless Decoding**. Previous methods typically derive the final mask directly after decoding video features, as exemplified by the use of an FCN decoder [55]. This approach neglects audio guidance information and omits object-level information during the decoding stage, potentially leading to segmentation errors in complex environments. For instance, in Figure 1 (b), the second frame of the video contains a violin, a piano, and people simultaneously. With audio containing only violin sounds and human singing, the target segmentation objects should be the person and the violin. However, due to the absence of audio constraints during the decoding phase, previous methods may erroneously segment the piano, influenced by the video’s focus on the front and back frames. Consequently, it is essential to introduce audio restrictions and provide object-level guidance information during the decoding phase.

To address the above limitations, we designed targeted modules:

(1) **Combinatorial-Dependence Fusion**. To comprehensively assess audio-visual combinatorial-dependence, we design to combine audio and video features from their respective temporal and spatial dimensions, followed by capturing this combination’s spatial-temporal dependence. Commonly, transformers are used to capture temporal dependencies; assuming a video frame dimension of $H \times W$, the merged feature dimension becomes $(H \times W + T)$. However, due to the substantial memory consumption associated with this encoder, we propose an innovative decoupling transformer that considerably reduces memory usage while allowing the extraction

of spatial-temporal interaction information between audio-audio, video-video, audio-video, and video-audio combinations.

(2) **Object-Aware Audio-Queried Decoding**. To enable attention focus on the object of interest, we propose an audio-queried decoder. Specifically, we apply an audio constraint to all object queries, allowing the model to leverage audio information to direct attention toward the desired object. These conditional queries serve as inputs for the model, which produces object-aware dynamic kernels to filter segmentation masks from feature maps.

On the whole, we propose a Combinatorial-Dependence Audio-Queried Transformer Network (CATR; Figure. 2), which contains two main components: Decoupled Audio-Visual Transformer Encoding Module (DAVT; detailed in Section. 4) and Audio-Queried Decoding Module (detailed in Section. 4.1). In encoding, we design an innovative decoupling block, which consists of two steps: initially, we merge audio and video features of corresponding frames while concurrently capturing their temporal information. Subsequently, we facilitate interaction between video features containing temporal information and audio features. By stacking decoupling blocks, we can efficiently capture audio-visual spatial-temporal correlations in a memory-efficient manner. In addition, Audio-Queried Decoder Module innovatively employ an audio constraint to all object queries to produce object-aware dynamic kernels to filter the segmentation of desired object. Moreover, we design a Blockwise-Encoded Gate to utilize all the features extracted from each encoder block. This Blockwise-Encoded Gate enables modeling of the overall distribution of all encoder blocks from a global perspective, thereby balancing the contributions of different encoder blocks.

We conduct extensive experiments on three popular benchmarks and achieve new state-of-the-art performance on all datasets with two backbones (On S4, CATR 84.4% \mathcal{J} / 91.3% \mathcal{F} vs. TPAV1 78.7%

$\mathcal{J} / 87.9\% \mathcal{F}$; On M3, CATR 61.8% $\mathcal{J} / 71\% \mathcal{F}$ vs. TPAVI 54% $\mathcal{J} / 64.5\% \mathcal{F}$). Our code and benchmark will be released.

Overall, our contributions are summarized as follows:

- We introduce an encoding-decoding framework CATR that presents a novel spatial-temporal audio-video fusion block to fully consider the audio-visual combinatorial dependence in a decoupled and memory-efficient manner.
- We propose the audio-constrained learnable queries to incorporate audio information comprehensively during decoding. These audio-constrained queries contain abundant object-level information that can select which object is being referred to segment. In addition, we introduce a Blockwise-Encoded Gate that allows for the selective fusion of features from different encoder blocks.
- We conduct extensive experiments on three popular benchmarks, and achieve new superior state-of-the-art performance on all three datasets with two backbones.

2 RELATED WORK

2.1 Video Object Segmentation (VOS)

The VOS task [38, 48] aims to segment the object of interest throughout the entire video sequence. It is divided into two settings: semi-supervised and unsupervised. For semi-supervised VOS [25, 47, 49, 52], the target object is decided given a one-shot mask of the first video frame. As for unsupervised VOS [15], it needs to segment all the primary objects automatically. Many excellent works are proposed and proven to achieve impressive segmentation performance. However, these fancy designs are limited to a single visual modality.

2.2 Audio-Visual Video Segmentation (AVVS)

The human ability to identify objects is not solely reliant on visual cues but also on auditory signals. For instance, the distinct sounds of a dog barking or a bird chirping are easily recognizable. This observation underscores the complementarity of audio and visual information. However, while speech-guided video segmentation is a more reliable means of distinguishing instance-level objects, sound can only provide information about object categories, making it a challenging task to locate and segment the object producing the sound. Zhou et al. [55] pioneered the audio-visual segmentation (AVVS) task and proposed a framework incorporating the TPAVI module, a groundbreaking approach for achieving pixel-level segmentation using audio information. Nonetheless, their framework's handling of multi-modal feature fusion and audio guidance was inadequate. Thus, we present a novel framework that addresses these limitations.

2.3 Vision Transformers

Transformer [36] was first introduced for sequence-to-sequence translation in natural language processing community and has achieved marvelous success in most computer vision tasks [7, 13, 16, 24] such as object detection [1, 57], tracking [4, 28, 33, 45] and segmentation [5, 17, 49, 53]. Unlike previous architectures, the Transformer relies entirely on the attention mechanism to draw dependencies between input and output. DETR [1], which utilizes

a non-auto-regressive Transformer, simplifies the traditional object detection pipeline while achieving performance comparable to that of CNN-based detectors [32]. Given a fixed set of learned object queries, DETR reasons about the global context of an image and the relations between its objects and then outputs a final set of detection predictions in parallel. VisTR [39] extends the idea behind DETR to video instance segmentation. It views the task as a direct end-to-end parallel sequence prediction problem. By supervising video instances at the sequence level as a whole, VisTR is able to output an ordered sequence of masks for each instance in a video directly. DeAOT [49] decouples the visual and identification features in hierarchical propagation [47] and achieves state-of-the-art performance in semi-supervised VOS. Inspired by these works, our work also relies on the query mechanism of Transformer but considers an additional modality, i.e., audio, as the object reference. Moreover, we propose an effective spatial-temporal fusion module to realize audio-guided video segmentation.

3 METHOD

3.1 Overview

Our pipeline for AVVS task can be formulated as encoding-decoding (depicted in Figure. 2). To address limitations in previous methods, such as inadequate correlation and vague reference, we carefully design two modules: the Decoupled Audio-Visual Transformer Encoding Module (DAVT; detailed in Section.4) and the Audio-Queried Decoding Module (detailed in Section.4.1). These modules enable effective audio-visual spatial-temporal connection and capture the object-level information to achieve more explicit reference, respectively. Moreover, we design a Blockwise-Encoded Gate to enable modeling of the overall distribution of all encoder blocks. In addition, CATR aims to output a pixel-level map of the object(s) that produce sound at the time of the image frame,

$$\{M_t\}_{t=1}^T = CATR(S_{t,v}, S_{t,a}), \quad (1)$$

where we denote the video sequence as $S = \{S_{t,v}, S_{t,a}\}_{t=1}^T$. Moreover, S_v denotes the visual sequence and S_a denotes the audio sequence. The predictions are denoted as $\{M_t\}_{t=1}^T$, $M_t \in \mathbb{R}^{H \times W}$.

4 DECOUPLED AUDIO-VISUAL TRANSFORMER

In contrast to existing methods that account for the video temporal information and audio-visual interaction separately, we propose a method that obtains the spatial-temporal combinatorial-dependence between audio-audio, video-video, audio-video, and video-audio in a novel decoupling memory-efficient manner.

Stack DAVT Blocks. To conserve memory, we designed the Decoupled Audio-Visual Transformer (DAVT). The DAVT block involves two steps. Initially, we combine the audio and video features of corresponding frames and capture their temporal information simultaneously. Subsequently, we interact processed video features with audio features, respectively.

For a video sequence S_v , we extract visual features after popular backbones and atrous spatial pyramid pooling [3] and obtain hierarchical visual feature maps. We denote the video features as $F_v \in \mathbb{R}^{T \times H \times W \times C}$, where T , H , W and C signifying the number of

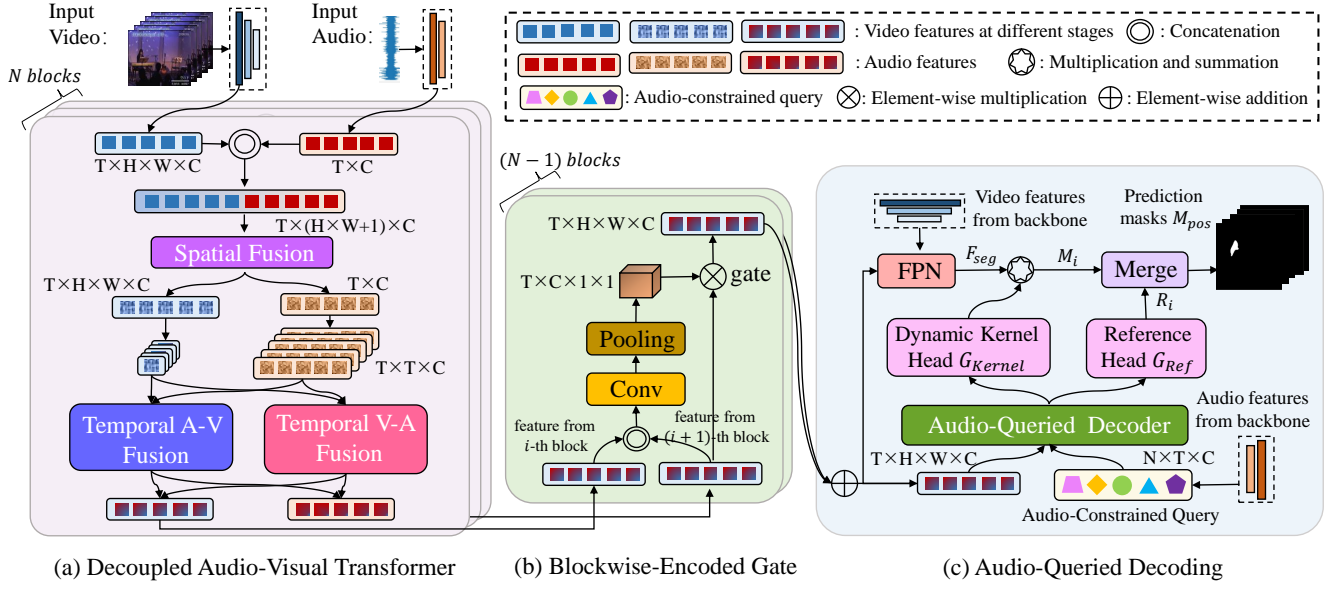


Figure 2: CATR employs an encoder-decoder structure. (a) In encoding, we merge audio and video features and capture their spatial-temporal combinatorial-dependencies. To conserve memory, we devise decoupling methods, utilizing temporal A-V and temporal V-A to fusion audio and video features. (b) To balance the contributions of multiple encoder blocks, we implement a blockwise gating method for utilizing all video features from each block. (c) In decoding, we introduce audio-constrained learnable queries, which harness audio features to extract object-level information, guiding target object segmentation.

frames, height, width, and channel, respectively. Given an audio sequence S_a , we employ a convolutional neural network VGGish [12] pre-trained on AudioSet [11] as backbone to extract audio features $F_a \in \mathbb{R}^{T \times d}$, where $d = 128$.

$$F_v^{l+1}, F_a^{l+1} = DAVT(F_v^l, F_a^l), \quad (2)$$

where $DAVT(\cdot)$ denotes the Decoupled Audio-Visual Transformer block, l denotes the l -th block. By stacking multiple DAVT blocks, we can effectively capture the spatial-temporal correlation between audio-audio, video-video, audio-video and video-audio in a memory-efficient manner.

Spatial Audio-Visual Fusion. To obtain the audio-visual overall dependence, the visual features F_v^l and audio features F_a^l are linearly projected to a shared dimension D . The video features of each frame are then flattened and separately concatenated with the audio embeddings, resulting in a set of T multi-modal sequences, each of shape $(H \times W + 1) \times D$.

$$\tilde{F}_v^l, \tilde{F}_a^l = SF(Concat(F_v^l, F_a^l)), \quad (3)$$

where $Concat(\cdot)$ denotes the concatenate operation, and $SF(\cdot)$ denotes the spatial audio-visual fusion function, which is employed as self-attention. Then we obtain the processed video feature \tilde{F}_v^l that contains the corresponding frame audio information. Similarly, the audio feature \tilde{F}_a^l contains the corresponding frame video information.

Temporal A-to-V Fusion. Employing a transformer-based encoder will consume a large amount of memory, so we use the decoupling

method to carry out Audio-to-Video (A-to-V) interaction and Video-to-Audio (V-to-A) interaction respectively.

$$\hat{F}_v^l, \hat{F}_a^l = TAV(\tilde{F}_v^l, \tilde{F}_a^l) = \text{Softmax} \left(\frac{\tilde{F}_v^l W^Q \cdot (\tilde{F}_a^l W^K)^T}{\sqrt{d_{\text{head}}}} \right) \tilde{F}_a^l W^V \quad (4)$$

where the $TAV(\cdot)$ denotes the Temporal Audio-to-Video Fusion, which is employed as multi-head attention [37]. In $TAV(\cdot)$, the query is the processed video feature \tilde{F}_v^l , and key is the audio feature \tilde{F}_a^l . Moreover, $W^Q, W^K, W^V \in \mathbb{R}^{C \times d_{\text{head}}}$ are learnable parameters.

Temporal V-to-A Fusion. Correspondingly, we also design a Temporal Video-to-Audio Fusion function $TVA(\cdot)$,

$$\tilde{F}_v^l, \tilde{F}_a^l = TVA(\tilde{F}_v^l, \tilde{F}_a^l) = \text{Softmax} \left(\frac{\tilde{F}_a^l W^Q \cdot (\tilde{F}_v^l W^K)^T}{\sqrt{d_{\text{head}}}} \right) \tilde{F}_v^l W^V, \quad (5)$$

where $TVA(\cdot)$ denotes the Temporal Video-to-Audio Fusion that is also employed as multi-head attention. In $TVA(\cdot)$, the query is the processed audio feature \tilde{F}_a^l and key is the video feature \tilde{F}_v^l .

After we obtain the video feature \tilde{F}_v^l that from $TVA(\cdot)$ and \hat{F}_v^l that from $TAV(\cdot)$, we merge the \tilde{F}_v^l and \hat{F}_v^l by element-wise adding and obtain the fully interacted video feature \bar{F}_v^l .

Blockwise-Encoded Gate. The existing method typically employs the features of the last encoder block alone as the decoder input, which is insufficient because the features of each encoder block contain varying degrees of multi-modal interaction information (see

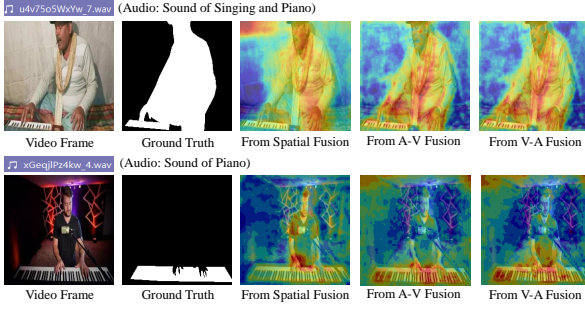


Figure 3: Attention maps generated from spatial fusion & temporal A-V/V-A fusions. Sample 1: target is person & piano; spatial fusion focuses on person, neglects piano; with temporal A-V/V-A fusions, the attention map accurately highlights both. Sample 2: target is the piano; spatial fusion wrongly emphasizes person, but temporal A-V/V-A maps correctly focus on piano. Consequently, we draw the conclusion that spatial fusion provides an initial integration of audio information, whereas temporal A-V and V-A fusions further consolidate this information to accurately identify the target object.

Figure 4). Thus, we design gate mechanisms to utilize all the features extracted from each encoder block and balance the contributions of different encoder blocks.

Suppose we have two video features \bar{F}_v^l and \bar{F}_v^{l+1} from different Spatial-Temporal Encoding blocks, we design a gate unit and G^{l+1} denotes the $(l+1)$ -th output vector,

$$\begin{aligned} G^{l+1} &= \text{Pool}(\text{Sigmoid}(\text{Conv}(\text{Concat}(\bar{F}_v^l, \bar{F}_v^{l+1})))), \\ F_v^{final} &= \text{Conv}(G^l \cdot \bar{F}_v^l + G^{l+1} \cdot \bar{F}_v^{l+1}), \end{aligned} \quad (6)$$

where $\text{Concat}(\cdot)$ denotes the concatenate operation, $\text{Conv}(\cdot)$ denotes the convolution layer, $\text{Sigmoid}(\cdot)$ denotes the sigmoid function and $\text{Pool}(\cdot)$ denotes the global average pooling. The output channel of $\text{Conv}(\cdot)$ is C , which means the resulted gate vector G^{l+1} has C different elements which correspond to C gate values (we set $C = 256$ here).

The gate values G^{l+1} is applied for weighting the different-blocks video features \bar{F}_v^l and \bar{F}_v^{l+1} . To obtain the final video encoding feature F_v^{final} , we fuse all the re-weighted features by element-wise addition and convolutional layers.

4.1 Audio-Queired Decoding

The existing methods fall short in effectively capturing object-level details and offering explicit information for cross-modal reasoning. To overcome this limitation, we propose audio-constrained queries, which impose an audio constraint on all object queries and generate object-aware dynamic kernels that filter target object segmentation masks from feature maps. Our approach aims to provide a comprehensive solution that enhances object recognition by incorporating audio signals into the process.

Audio-Constrained Query. We hierarchically fuse the final video feature F_v^{final} and the multi-layer features from backbone with an FPN-like [19] decoder, then we obtain the semantically-rich video feature maps $F_{seg} = \{f_{seg,t}\}_{t=1}^T$, where $f_{seg,t} \in \mathbb{R}^{\frac{H}{8} \times \frac{W}{8} \times C}$.

To capture the object-level information comprehensively, we devised a set of N learnable queries. These queries, along with the audio feature, were fed into the decoder embedding and position embedding in the transformer, resulting in queries with abundant object-level information. Next, we use two-layer dynamic kernels $\mathcal{G}_{\text{kernel}}$ to generate a corresponding sequence segmentation for each query. Finally, the binary segmentation masks are generated by performing dynamic convolution between the conditional convolutional weights and their corresponding feature maps:

$$M_i = \{F_{seg} * \omega_i\}_{i=1}^N, \quad (7)$$

where $M_i \in \mathbb{R}^{N \times \frac{H}{8} \times \frac{W}{8}}$ denotes the segmentation mask with N queries. ω_i and F_{seg} denote the i -th dynamic kernel weights and its exclusive feature map, respectively.

Query Matching. During the training process, we need to determine which of the predicted sequences best fits the referred object. Here, we denote each ground-truth sequence as $y = (M, R) = (\{M_t\}_{t=1}^T, \{R_t\}_{t=1}^T)$, where M denotes the ground-truth mask and R denotes a probability scalar indicating whether the instance corresponds to the referred object and this object is visible in the current frame. In addition, we denote the prediction set as $\hat{y} = \{\hat{y}_i\}_{i=1}^N$, where $\hat{y}_i = (\{\hat{M}_{i,t}\}_{t=1}^T, \{\hat{R}_{i,t}\}_{t=1}^T)$.

To find the best prediction from N conditional queries, we use a reference head \mathcal{G}_{Ref} , which consists of a single linear layer followed by a softmax layer. Then we obtain the positive sample by minimizing the matching cost:

$$\begin{aligned} \hat{y}_{\text{pos}} &= \arg \min_{\hat{y}_i \in \hat{y}} C_{\text{match}}(y, \hat{y}_i), \\ C_{\text{match}}(y, \hat{y}_i) &= C_{\text{dice}}(M, \hat{M}_i) + C_{\text{ref}}(R, \hat{R}_i) \end{aligned} \quad (8)$$

where \hat{y}_{pos} denotes the permutation in N conditional queries with the lowest total cost. C_{dice} supervises the predicted mask sequence using the ground-truth mask sequence by the Dice coefficients [29], and C_{ref} supervises the reference predictions using the corresponding ground-truth reference identity by cross-entropy.

4.2 Loss and Inference

We consider both mask and reference identity, and we define our loss function as follows:

$$\begin{aligned} \mathcal{L}(y, \hat{y}_i) &= \mathcal{L}_{\text{Mask}}(M_i, \hat{M}_i) + \mathcal{L}_{\text{Ref}}(R_i, \hat{R}_i) \\ &= \lambda_d \mathcal{L}_{\text{Dice}}(M_i, \hat{M}_i) + \lambda_f \mathcal{L}_{\text{Focal}}(M_i, \hat{M}_i) + \lambda_r \mathcal{L}_{\text{Ref}}(R_i, \hat{R}_i) \end{aligned} \quad (9)$$

where $\mathcal{L}_{\text{Mask}}$ ensures mask alignment between the predicted and ground-truth, and \mathcal{L}_{Ref} supervises the reference identity predictions. In addition, $\mathcal{L}_{\text{Mask}}$ is implemented by a combination of the Dice [29] and the per-pixel Focal [20] loss functions, and \mathcal{L}_{Ref} is implemented by a cross-entropy term.

For inference, CATR will predict N object sequences. For each sequence, we obtain the predicted reference probabilities and the reference score set $P = \{p_i\}_{i=1}^N$. We select the object sequence with the highest score and its index is denoted as R_{pos} ,

$$R_{\text{pos}} = \arg \max_{i \in \{1, 2, \dots, N\}} p_i \quad (10)$$

Finally, we return the final mask M_{pos} that corresponds to R_{pos} .

Task	Method	Backbone	S4		M3	
			$\mathcal{M}_{\mathcal{J}}$	$\mathcal{M}_{\mathcal{F}}$	$\mathcal{M}_{\mathcal{J}}$	$\mathcal{M}_{\mathcal{F}}$
SSL	LVS [2]	resnet18	37.9	51	29.5	33
	MSSL [30]	resnet18	44.9	66.3	26.1	36.3
VOS	3DC [26]	resnet152	57.1	75.9	36.9	50.3
	SST [9]	resnet101	66.3	80.1	42.6	57.2
SOD	iGAN [27]	resnet50	61.6	77.8	42.9	54.4
	LGVt [51]	swin	74.9	87.3	40.7	59.3
AVVS	TPAVI [55]	resnet50	72.8	84.8	47.9	57.8
		PVT-v2	78.7	87.9	54.0	64.5
	CATR	resnet50	74.8	86.6	52.8	65.3
		PVT-v2	81.4	89.6	59.0	70.0
	CATR*	resnet50	74.9	87.1	53.1	65.6
		PVT-v2	84.4	91.3	62.7	74.5

Table 1: Quantitative comparisons on AVSBench-object datasets (single-source, S4; multi-source, M3). Blue indicates the best performance with resnet backbone, while red indicates the best performance among all settings. * denotes that the training datasets are supplemented annotation with AOT.

Task	Method	Backbone	AVSS	
			$\mathcal{M}_{\mathcal{J}}$	$\mathcal{M}_{\mathcal{F}}$
VOS	3DC [26]	resnet18	17.3	21.6
	AOT [47]	resnet50	25.4	31.0
AVSS	TPAVI [54]	PVT-v2	29.8	35.2
	CATR	PVT-v2	32.8	38.5

Table 2: Quantitative comparisons on AVSBench-semantic datasets (AVSS). Red indicates the best performance.

5 EXPERIMENT

5.1 Implementation Details

Datasets. We train and validate our model on three datasets: Semi-supervised Single-sound Source Segmentation (S4), Fully-supervised Multiple-sound Source Segmentation (M3), and Fully-supervised Audio-Visual Semantic Segmentation (AVSS). S4 and M3 datasets provide binary segmentation maps identifying the pixels of sound-ing objects, while the AVSS dataset offers semantic segmentation maps as labels. The S4 dataset contains audio samples with a single target object, supplying ground-truth solely for the initial frame during training. Evaluation necessitates predictions for all video frames in the test set. In contrast, both M3 and AVSS datasets contain audio samples with multiple target objects and furnish ground-truth data for all frames throughout the training phase.

Training Details. We conduct training and evaluation on S4, M3 and AVSS datasets, with the backbone ResNet-50 and Pyramid Vi-sion Transformer (PVT-v2). The channel size of the spatial-temporal encoding module is set to $C = 256$. We use the VGGish model to extract audio features and use the Adam optimizer with a learning rate of $1e-5$ for the fully-supervised M3 settings, $1e-4$ for the semi-supervised S4 and the fully-supervised AVSS settings. The batch size is set to 4 and the number of audio-constrained queries is set

PVT-v2	M3		S4	
	$\mathcal{M}_{\mathcal{J}}$	$\mathcal{M}_{\mathcal{F}}$	$\mathcal{M}_{\mathcal{J}}$	$\mathcal{M}_{\mathcal{F}}$
Baseline	51.2	63.3	77.9	87.6
(+) Annotation	53.1	64.7	79.1	88.5
(+) Decoupled A-V Transformer	57.7	68.6	82.6	90.1
(+) Blockwise-Encoded Gate	60.8	70.3	83.8	91.1
(+) Audio-queried Decoding	62.7	74.5	84.4	91.3

Table 3: Ablation analysis on the M3 and S4 dataset with PVT-v2 backbone.

as 50. On S4, we set the training epoch as 25, and On M3 and AVSS, we set the training epoch as 100.

Evaluation Metrics. We use standard metrics Jaccard index [10] \mathcal{J} and F-score \mathcal{F} as the evaluation metrics, where \mathcal{J} and \mathcal{F} measure the region similarity and contour accuracy, respectively. In our experiment, we use $\mathcal{M}_{\mathcal{J}}$ and $\mathcal{M}_{\mathcal{F}}$ to denote the mean metric values over the whole dataset.

5.2 Comparison

Compare with Other Tasks. Audio-visual video segmentation (AVVS) is a relatively new and emerging task, first introduced by [55], which aims to segment target objects in videos based on corresponding sounds. Although some well-established tasks, such as sound source localization (SSL), video object segmentation (VOS) and salient object detection (SOD) can perform video object seg-mentation, we utilize state-of-the-art methods from these related tasks as a comparative benchmark for our experiments. As evi-dent in Table 1, there exists a significant performance gap between SSL-based methods and our CATR, primarily due to the lack of pixel-level results in SSL. Furthermore, our model demonstrates a clear advantage over video object segmentation (VOS) and salient object detection (SOD) methods on both S4 and M3 datasets. This superior performance can be attributed to the fact that VOS and SOD are single-mode tasks and do not utilize sound information. In summary, the comparison with SOTA methods from related tasks substantiates the exceptional performance of our model in AVVS.

Compare with SOTA TPAVI. Our proposed CATR outperforms the previous SOTA TPAVI on all datasets (S4, M3 and AVSS) with two backbones (see Figure 1 and 2). This improvement is due to the integration of the decoupled audio-visual transformer encod-ing module (DAVT) and the object-aware audio-queried decoding module. The DAVT block captures the combinatorial dependence of audio and video, combining audio and video in the space dimen-sion to capture the temporal characteristics of this multi-modal combination. Compared to the previous model that considered the audio-visual temporal and interactive features independently, the combinatorial dependence we obtained is better equipped to locate the referred object. Additionally, our object-aware audio-queried decoder utilizes multiple queries containing rich audio cues and object-level information, providing more accurate object segmen-tation and target location compared to the previous model’s decoding directly. By considering both object-level and audio-constrained decoding, our model achieves more precise results.

Compare with the Processed Data. Limited datasets exist for audio-visual video segmentation, leading [55] to introduce AVSBench-object datasets first. Among these, S4 represents a semi-supervised

Resnet50	M3		S4	
	M_J	M_F	M_J	M_F
TPAVI w audio	47.9	57.8	72.8	84.8
CATR w/o audio	36.4	51.4	73.2	84.6
CATR w audio	52.1	64.6	74.1	86.1

PVT-v2	M3		S4	
	M_J	M_F	M_J	M_F
TPAVI w audio	54.0	64.5	78.7	87.9
CATR w/o audio	43.9	57.6	80.7	89.1
CATR w audio	62.7	74.5	84.4	91.3

Table 4: Comparison between TPAVI with audio information and CATR without audio information.

PVT-v2	M3	
	M_J	M_F
CATR	62.7	74.5
w/o spatial fusion	59.7	70.7
w/o temporal A-V fusion	58.4	69.8
w/o temporal V-A fusion	61.8	71.0

Table 5: Ablation analysis of spatial-temporal encoding.

Gate Channel	M3		S4	
	M_J	M_F	M_J	M_F
2	58.4	69.8	83.5	90.8
64	61.8	70.9	83.9	91.1
128	62.1	72.9	84.2	91.2
256	62.7	74.5	84.4	91.3

Table 6: Analysis of the number of channels in Blockwise-Encoded Gate with PVT-v2 backbone.

learning task, providing ground-truth for the first frame in the training set. To maximize dataset utility without incurring additional labor, we devised a complementary approach for S4 and M3 datasets. Specifically, during M3 training, we employed AOT [47] to predict unlabeled frames of the S4 training set, using these predictions as ground-truth for the AVVS task. Concurrently, we preserved the same setting as TPAVI, implementing semi-supervised training for the S4 dataset and fully supervised training for the M3 dataset.

Table 1’s experimental results demonstrate that our model’s performance on the original dataset (CATR) surpasses the previous state-of-the-art TPAVI, and the supplementary labeling method (CATR*) further enhances the model’s effectiveness.

5.3 Contribution of The Core Components

Table 3 demonstrates the contributions of each proposed module to the overall performance enhancement in CATR, utilizing PVT-v2 and ASPP as encoding and expanded fused feature maps as decoding in the baseline. Given the limited original training samples, it is essential to maximize the use of available data. We augment the two training sets, respecting their semi-supervised and fully supervised configurations, due to the similarity of their segmentation objectives. Specifically, we incorporated M3 video data into the S4 training set and supplemented the S4 training set with AOT-generated ground-truth when training the M3 dataset. The second

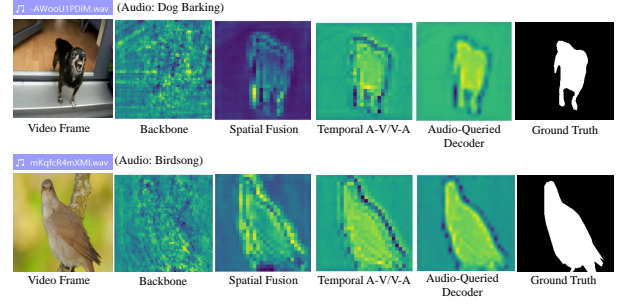


Figure 4: Visualization of video features after processing at each stage. We observed that the initial features, generated by the backbone network, appeared indistinct. However, the video features progressively aligned with the desired segmentation object after the spatial-temporal encoding module.

row in Table 3 indicates that our additional annotation improves the performance of both M3 and S4 datasets.

Furthermore, our experiments reveal that the decoupled audio-visual transformer encoding, blockwise-encoded gate, and audio-queried decoding modules significantly enhance the model’s performance. Notably, the audio-queried decoding module exhibits a more substantial improvement in the M3 dataset than in the S4 dataset (M_J is up 6.5 vs. 0.6). This is attributable to the multiple objectives in M3 dataset videos, which complicate segmentation target identification. The audio-constrained query contains rich object-level information and guides the segmentation effectively.

The Impact of Decoupled A-V Transformer Encoding. We developed a decoupled spatial-temporal encoding block consisting of three components. Initially, we integrated audio and video features in the spatial domain using a spatial fusion method, capturing the temporal dependence of this combination. Subsequently, the spatially fused features were processed through both the temporal A-V and temporal V-A modules. Table 5 demonstrates the contributions of each component to overall performance, highlighting the critical role played by the temporal A-V module. We attribute its significance to the predominant use of video features in the final decoding process, where video features serve as the key and value within the temporal A-V module, preserving crucial video information. To further illustrate this, we examined the attention maps of features processed by the spatial-temporal encoding block, depicted in Figure 3. The initial spatial fusion attention map appears scattered, particularly in the second example, indicating insufficient integration of audio guidance information. In contrast, attention maps for both temporal A-V and temporal V-A modules are more precise and focused, with the temporal A-V map in the second example almost exclusively centered on the piano, underscoring its importance.

The Impact of Blockwise-Encoded Gate. To optimize the contributions from each encoder block, the Blockwise-Encoded Gate was devised to fully harness the potential of the individual encoders’ features. Table 3 demonstrates the enhancement in model performance when incorporating the Blockwise-Encoded Gate. Table 6 examines the influence of varying the number of channels within the Blockwise-Encoded Gate, where channels denote the quantity obtained after passing through a convolutional layer, reflecting the designated number of weights. The experimental findings indicate

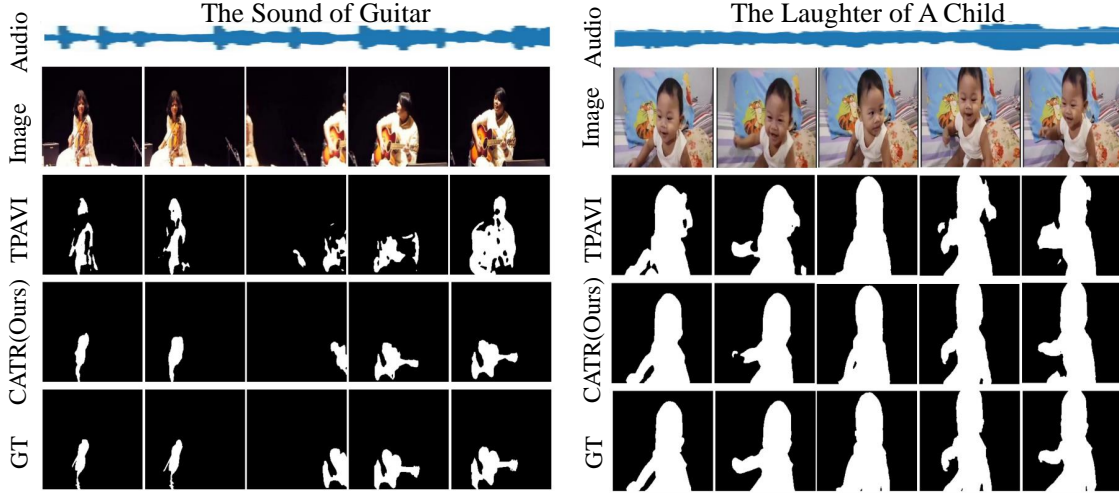


Figure 5: Comparative analysis of the TPAVI method and our proposed CATR. We present two qualitative examples from the M3 and S4 datasets. The M3 dataset example (left) demonstrates TPAVI’s inability to detect the transition of auditory objects, such as from a violin to a guitar, whereas CATR accurately predicts these changes in alignment with the audio signal. In S4 example (right), CATR exhibits better performance on pixel-level segmentation in the presence of a complex background.

that optimal performance is achieved with 256 channels, corresponding to our feature dimension. This suggests that assigning a weight to each feature channel enables the model to effectively account for the proportional contribution of each feature.

The Impact of Audio-Queried Decoding. In the decoding phase, we developed N learnable queries incorporating auditory cues and comprehensive object-level information. We employed the C_{match} function to select the query optimally aligned with the audio features, which served as the final mask. As demonstrated in Table 3, our audio-constrained query decoding approach substantially enhances the model’s performance. Previous models neglect audio information in their decoding stages, resulting in segmentation outcomes predominantly influenced by adjacent video frames. Consequently, by emphasizing audio features during the decoding process, we effectively improve overall performance.

5.4 The Impact of Audio Signals

The enhanced performance of CATR prompts an inquiry: Does this improvement stem from a superior comprehension of pixel-level video features or more effective utilization of audio features? To investigate, we conducted an experiment that removed audio features from the Spatial-Temporal Encoding Module and applied self-attention to video features. Additionally, we replaced learnable queries, originally constrained by audio, with video features in the decoding module. Table 4 presents the results of CATR without audio. These findings reveal that (1) our model effectively leverages audio features, as evidenced by the significant improvement in the M3 dataset when comparing CATR with and without audio (M_J is 0.627 vs. 0.439 with PVT-v2); and (2) our model demonstrates a more advanced understanding of pixel-level video features, as shown by the superior performance in the S4 dataset, even without employing audio information, surpassing the previous state-of-the-art TPAVI (M_J is 0.807 vs. 0.787 with PVT-v2).

6 CONCLUSION

We introduce a novel Combinatorial-Dependence Audio-Queried Transformer (CATR) framework that achieves state-of-the-art performance on all three datasets using two backbones. Unlike previous methods that treated temporal video information and audio-visual interaction separately, our proposed combinatorial dependence fusion approach comprehensively accounts for the spatial-temporal dependencies of audio-visual combination. Additionally, we propose the audio-constrained learnable queries to incorporate audio information comprehensively during decoding. These queries contain object-level information that can select which object is being referred to segment. To further enhance performance, we introduce a blockwise-encoded gate that balances contributions from multiple encoder blocks. Our experimental results demonstrate the significant impact of these novel components on overall performance.

Limitations: Objects with similar auditory characteristics can confound video segmentation outcomes when they coexist within a single frame. To address this challenge, we plan to explore the refinement of audio feature pre-processing in future research. **Broader Impact:** The exceptional performance of CATR enables its practical implementation in audio-guided video segmentation applications. These applications include utilizing auditory cues to accentuate objects in augmented and virtual reality environments and generating pixel-level object maps for surveillance inspections. We expect that our research will contribute to practical applications of audio-guided video segmentation.

ACKNOWLEDGMENTS

This work was supported by the Fundamental Research Funds for the Central Universities (No. 226-2023-00048), the National Key Research & Development Project of China (2021ZD0110700), and the National Natural Science Foundation of China (U19B2043, 61976185).

REFERENCES

- [1] Nicolas Carion, Francisco Massa, Gabriel Synnaeve, Nicolas Usunier, Alexander Kirillov, and Sergey Zagoruyko. 2020. End-to-End Object Detection with Transformers. In *Computer Vision - ECCV 2020 - 16th European Conference, Glasgow, UK, August 23–28, 2020, Proceedings, Part I (Lecture Notes in Computer Science, Vol. 12346)*, Andrea Vedaldi, Horst Bischof, Thomas Brox, and Jan-Michael Frahm (Eds.). Springer, 213–229. https://doi.org/10.1007/978-3-030-58452-8_13
- [2] Honglie Chen, Weidi Xie, Triantafyllos Afouras, Arsha Nagrani, Andrea Vedaldi, and Andrew Senior. 2021. Localizing visual sounds the hard way. In *Proceedings of the IEEE/CVF Conference on Computer Vision and Pattern Recognition*. 16867–16876.
- [3] Liang-Chieh Chen, George Papandreou, Iasonas Kokkinos, Kevin Murphy, and Alan L. Yuille. 2017. Deeplab: Semantic image segmentation with deep convolutional nets, atrous convolution, and fully connected crfs. *IEEE transactions on pattern analysis and machine intelligence* 40, 4 (2017), 834–848.
- [4] Xin Chen, Bin Yan, Jiawen Zhu, Dong Wang, Xiaoyun Yang, and Huchuan Lu. 2021. Transformer Tracking. In *IEEE Conference on Computer Vision and Pattern Recognition, CVPR 2021, virtual, June 19–25, 2021*. Computer Vision Foundation / IEEE, 8126–8135. <https://doi.org/10.1109/CVPR46437.2021.00803>
- [5] Bowen Cheng, Alexander G. Schwing, and Alexander Kirillov. 2021. Per-Pixel Classification is Not All You Need for Semantic Segmentation. In *Advances in Neural Information Processing Systems 34: Annual Conference on Neural Information Processing Systems 2021, NeurIPS 2021, December 6–14, 2021, virtual*, Marc' Aurelio Ranzato, Alina Beygelzimer, Yann N. Dauphin, Percy Liang, and Jennifer Wortman Vaughan (Eds.). 17864–17875. <https://proceedings.neurips.cc/paper/2021/hash/950a4152c2b4aa3ad78bdd6b366cc179-Abstract.html>
- [6] Yangming Cheng, Liulei Li, Yuanyou Xu, Xiaodi Li, Zongxin Yang, Wenguan Wang, and Yi Yang. 2023. Segment and track anything. *arXiv preprint arXiv:2305.06558* (2023).
- [7] Alexey Dosovitskiy, Lucas Beyer, Alexander Kolesnikov, Dirk Weissenborn, Xi-aohua Zhai, Thomas Unterthiner, Mostafa Dehghani, Matthias Minderer, Georg Heigold, Sylvain Gelly, Jakob Uszkoreit, and Neil Houlsby. 2021. An Image is Worth 16x16 Words: Transformers for Image Recognition at Scale. In *9th International Conference on Learning Representations, ICLR 2021, Virtual Event, Austria, May 3–7, 2021*. OpenReview.net. <https://openreview.net/forum?id=YicbFdNTTy>
- [8] Bin Duan, Hao Tang, Wei Wang, Ziliang Zong, Guowei Yang, and Yan Yan. 2021. Audio-visual event localization via recursive fusion by joint co-attention. In *Proceedings of the IEEE/CVF Winter Conference on Applications of Computer Vision*. 4013–4022.
- [9] Brendan Duke, Abdalla Ahmed, Christian Wolf, Parham Aarabi, and Graham W Taylor. 2021. Sstvos: Sparse spatiotemporal transformers for video object segmentation. In *Proceedings of the IEEE/CVF Conference on Computer Vision and Pattern Recognition*. 5912–5921.
- [10] Mark Everingham, Luc Van Gool, Christopher KI Williams, John Winn, and Andrew Zisserman. 2010. The pascal visual object classes (voc) challenge. *International journal of computer vision* 88 (2010), 303–338.
- [11] Jort F Gemmeke, Daniel PW Ellis, Dylan Freedman, Aren Jansen, Wade Lawrence, R Channing Moore, Manoj Plakal, and Marvin Ritter. 2017. Audio set: An ontology and human-labeled dataset for audio events. In *2017 IEEE international conference on acoustics, speech and signal processing (ICASSP)*. IEEE, 776–780.
- [12] Shawn Hershey, Sourish Chaudhuri, Daniel P. W. Ellis, Jort F. Gemmeke, Aren Jansen, R. Channing Moore, Manoj Plakal, Devin Platt, Rif A. Saurous, Bryan Seybold, Malcolm Slaney, Ron J. Weiss, and Kevin W. Wilson. 2017. CNN architectures for large-scale audio classification. In *2017 IEEE International Conference on Acoustics, Speech and Signal Processing, ICASSP 2017, New Orleans, LA, USA, March 5–9, 2017*. IEEE, 131–135. <https://doi.org/10.1109/ICASSP.2017.7952132>
- [13] Aishwarya Kamath, Mannat Singh, Yann LeCun, Gabriel Synnaeve, Ishan Misra, and Nicolas Carion. 2021. MDETR - Modulated Detection for End-to-End Multi-Modal Understanding. In *2021 IEEE/CVF International Conference on Computer Vision, ICCV 2021, Montreal, QC, Canada, October 10–17, 2021*. IEEE, 1760–1770. <https://doi.org/10.1109/ICCV48922.2021.00180>
- [14] Alexander Kirillov, Eric Mintun, Nikhila Ravi, Hanzi Mao, Chloe Rolland, Laura Gustafson, Tete Xiao, Spencer Whitehead, Alexander C Berg, Wan-Yen Lo, et al. 2023. Segment anything. *arXiv preprint arXiv:2304.02643* (2023).
- [15] Liulei Li, Wenguan Wang, Tianfei Zhou, Jianwu Li, and Yi Yang. 2023. Unified Mask Embedding and Correspondence Learning for Self-Supervised Video Segmentation. In *Proceedings of the IEEE/CVF Conference on Computer Vision and Pattern Recognition*. 18706–18716.
- [16] Wenhui Li, Song Yang, Qiang Li, Xuanya Li, and An-An Liu. 2023. Commonsense-Guided Semantic and Relational Consistencies for Image-Text Retrieval. *IEEE Transactions on Multimedia* (2023).
- [17] Chen Liang, Wenguan Wang, Jiaxu Miao, and Yi Yang. 2022. Gmmseg: Gaussian mixture based generative semantic segmentation models. In *Advances in Neural Information Processing Systems*, Vol. 35. 31360–31375.
- [18] Chen Liang, Wenguan Wang, Tianfei Zhou, Jiaxu Miao, Yawei Luo, and Yi Yang. 2023. Local-Global Context Aware Transformer for Language-Guided Video Segmentation. *IEEE Transactions on Pattern Analysis and Machine Intelligence* 45, 8 (2023), 10055–10069. <https://doi.org/10.1109/TPAMI.2023.3262578>
- [19] Tsung-Yi Lin, Piotr Dollár, Ross B. Girshick, Kaiming He, Bharath Hariharan, and Serge J. Belongie. 2017. Feature Pyramid Networks for Object Detection. In *2017 IEEE Conference on Computer Vision and Pattern Recognition, CVPR 2017, Honolulu, HI, USA, July 21–26, 2017*. IEEE Computer Society, 936–944. <https://doi.org/10.1109/CVPR.2017.106>
- [20] Tsung-Yi Lin, Priya Goyal, Ross Girshick, Kaiming He, and Piotr Dollár. 2017. Focal loss for dense object detection. In *Proceedings of the IEEE international conference on computer vision*. 2980–2988.
- [21] Yan-Bo Lin, Yu-Jhe Li, and Yu-Chiang Frank Wang. 2019. Dual-modality seq2seq network for audio-visual event localization. In *ICASSP 2019-2019 IEEE International Conference on Acoustics, Speech and Signal Processing (ICASSP)*. IEEE, 2002–2006.
- [22] Yan-Bo Lin, Hung-Yu Tseng, Hsin-Ying Lee, Yen-Yu Lin, and Ming-Hsuan Yang. 2021. Exploring cross-video and cross-modality signals for weakly-supervised audio-visual video parsing. *Advances in Neural Information Processing Systems* 34 (2021), 11449–11461.
- [23] Yan-Bo Lin and Yu-Chiang Frank Wang. 2020. Audiovisual transformer with instance attention for audio-visual event localization. In *Proceedings of the Asian Conference on Computer Vision*.
- [24] Ze Liu, Yutong Lin, Yue Cao, Han Hu, Yixuan Wei, Zheng Zhang, Stephen Lin, and Baining Guo. 2021. Swin Transformer: Hierarchical Vision Transformer using Shifted Windows. In *2021 IEEE/CVF International Conference on Computer Vision, ICCV 2021, Montreal, QC, Canada, October 10–17, 2021*. IEEE, 9992–10002. <https://doi.org/10.1109/ICCV48922.2021.00986>
- [25] Xiankai Lu, Wenguan Wang, Martin Danelljan, Tianfei Zhou, Jianbing Shen, and Luc Van Gool. 2020. Video object segmentation with episodic graph memory networks. In *Computer Vision–ECCV 2020: 16th European Conference, Glasgow, UK, August 23–28, 2020, Proceedings, Part III 16*. Springer, 661–679.
- [26] Sabarinath Mahadevan, Ali Athar, Aljoša Ošep, Sebastian Hennen, Laura Leal-Taixé, and Bastian Leibe. 2020. Making a case for 3d convolutions for object segmentation in videos. *arXiv preprint arXiv:2008.11516* (2020).
- [27] Yuxin Mao, Jing Zhang, Zhexiong Wan, Yuchao Dai, Aixuan Li, Yunqiu Lv, Xinyu Tian, Deng-Ping Fan, and Nick Barnes. 2021. Transformer transforms salient object detection and camouflaged object detection. *arXiv preprint arXiv:2104.10127* (2021).
- [28] Tim Meinhardt, Alexander Kirillov, Laura Leal-Taixé, and Christoph Feichtenhofer. 2022. TrackFormer: Multi-Object Tracking with Transformers. In *IEEE/CVF Conference on Computer Vision and Pattern Recognition, CVPR 2022, New Orleans, LA, USA, June 18–24, 2022*. IEEE, 8834–8844. <https://doi.org/10.1109/CVPR52688.2022.00864>
- [29] Fausto Milletari, Nassir Navab, and Seyed-Ahmad Ahmadi. 2016. V-net: Fully convolutional neural networks for volumetric medical image segmentation. In *2016 fourth international conference on 3D vision (3DV)*. Ieee, 565–571.
- [30] Rui Qian, Di Hu, Heinrich Dinkel, Mengyue Wu, Ning Xu, and Weiyao Lin. 2020. Multiple sound sources localization from coarse to fine. In *Computer Vision–ECCV 2020: 16th European Conference, Glasgow, UK, August 23–28, 2020, Proceedings, Part XX 16*. Springer, 292–308.
- [31] Janani Ramaswamy and Sukhendu Das. 2020. See the sound, hear the pixels. In *Proceedings of the IEEE/CVF Winter Conference on Applications of Computer Vision*. 2970–2979.
- [32] Shaoqing Ren, Kaiming He, Ross B. Girshick, and Jian Sun. 2017. Faster R-CNN: Towards Real-Time Object Detection with Region Proposal Networks. *IEEE Trans. Pattern Anal. Mach. Intell.* 39, 6 (2017), 1137–1149. <https://doi.org/10.1109/TPAMI.2016.2577031>
- [33] Peize Sun, Yi Jiang, Rufeng Zhang, Enze Xie, Jinkun Cao, Xinting Hu, Tao Kong, Zehuan Yuan, Changhu Wang, and Ping Luo. 2020. TransTrack: Multiple-Object Tracking with Transformer. *CoRR abs/2012.15460* (2020). [arXiv:2012.15460](https://arxiv.org/abs/2012.15460)
- [34] Yapeng Tian, Dingzeyu Li, and Chenliang Xu. 2020. Unified multisensory perception: Weakly-supervised audio-visual video parsing. In *Computer Vision–ECCV 2020: 16th European Conference, Glasgow, UK, August 23–28, 2020, Proceedings, Part III 16*. Springer, 436–454.
- [35] Yapeng Tian, Jing Shi, Bochen Li, Zhiyao Duan, and Chenliang Xu. 2018. Audio-visual event localization in unconstrained videos. In *Proceedings of the European Conference on Computer Vision (ECCV)*. 247–263.
- [36] Ashish Vaswani, Noam Shazeer, Niki Parmar, Jakob Uszkoreit, Llion Jones, Aidan N. Gomez, Lukasz Kaiser, and Illia Polosukhin. 2017. Attention is All you Need. In *Advances in Neural Information Processing Systems 30: Annual Conference on Neural Information Processing Systems 2017, December 4–9, 2017, Long Beach, CA, USA*, Isabelle Guyon, Ulrike von Luxburg, Samy Bengio, Hanna M. Wallach, Rob Fergus, S. V. N. Vishwanathan, and Roman Garnett (Eds.). 5998–6008. <https://proceedings.neurips.cc/paper/2017/hash/3f5ee243547dee91fbd053c1c4a845aa-Abstract.html>
- [37] Ashish Vaswani, Noam Shazeer, Niki Parmar, Jakob Uszkoreit, Llion Jones, Aidan N Gomez, Lukasz Kaiser, and Illia Polosukhin. 2017. Attention is all you need. *Advances in neural information processing systems* 30 (2017).
- [38] Wenguan Wang, Tianfei Zhou, Fatih Porikli, David Crandall, and Luc Van Gool. 2021. A survey on deep learning technique for video segmentation. *arXiv e-prints*

- (2021), arXiv-2107.
- [39] Yuqing Wang, Zhaoliang Xu, Xinlong Wang, Chunhua Shen, Baoshan Cheng, Hao Shen, and Huaxia Xia. 2021. End-to-End Video Instance Segmentation With Transformers. In *IEEE Conference on Computer Vision and Pattern Recognition, CVPR 2021, virtual, June 19-25, 2021*. Computer Vision Foundation / IEEE, 8741–8750. <https://doi.org/10.1109/CVPR46437.2021.00863>
 - [40] Jiannan Wu, Yi Jiang, Peize Sun, Zehuan Yuan, and Ping Luo. 2022. Language as queries for referring video object segmentation. In *Proceedings of the IEEE/CVF Conference on Computer Vision and Pattern Recognition*. 4974–4984.
 - [41] Yu Wu and Yi Yang. 2021. Exploring heterogeneous clues for weakly-supervised audio-visual video parsing. In *Proceedings of the IEEE/CVF Conference on Computer Vision and Pattern Recognition*. 1326–1335.
 - [42] Yu Wu, Linchao Zhu, Yan Yan, and Yi Yang. 2019. Dual attention matching for audio-visual event localization. In *Proceedings of the IEEE/CVF international conference on computer vision*. 6292–6300.
 - [43] Haoming Xu, Runhao Zeng, Qingyao Wu, Minghui Tan, and Chuang Gan. 2020. Cross-modal relation-aware networks for audio-visual event localization. In *Proceedings of the 28th ACM International Conference on Multimedia*. 3893–3901.
 - [44] Hanyu Xuan, Zhenyu Zhang, Shuo Chen, Jian Yang, and Yan Yan. 2020. Cross-modal attention network for temporal inconsistent audio-visual event localization. In *Proceedings of the AAAI Conference on Artificial Intelligence*, Vol. 34. 279–286.
 - [45] Bin Yan, Houwen Peng, Jianlong Fu, Dong Wang, and Huchuan Lu. 2021. Learning Spatio-Temporal Transformer for Visual Tracking. In *2021 IEEE/CVF International Conference on Computer Vision, ICCV 2021, Montreal, QC, Canada, October 10-17, 2021*. IEEE, 10428–10437. <https://doi.org/10.1109/ICCV48922.2021.01028>
 - [46] Yi Yang, Yueting Zhuang, and Yunhe Pan. 2021. Multiple knowledge representation for big data artificial intelligence: framework, applications, and case studies. *Frontiers of Information Technology & Electronic Engineering* 22, 12 (2021), 1551–1558.
 - [47] Zongxin Yang, Yunchao Wei, and Yi Yang. 2021. Associating objects with transformers for video object segmentation. *Advances in Neural Information Processing Systems* 34 (2021), 2491–2502.
 - [48] Zongxin Yang, Yunchao Wei, and Yi Yang. 2021. Collaborative video object segmentation by multi-scale foreground-background integration. *TPAMI* 44, 9 (2021), 4701–4712.
 - [49] Zongxin Yang and Yi Yang. 2022. Decoupling Features in Hierarchical Propagation for Video Object Segmentation. In *NeurIPS*.
 - [50] Jiashuo Yu, Ying Cheng, Rui-Wei Zhao, Rui Feng, and Yuejie Zhang. 2022. Mm-pyramid: Multimodal pyramid attentional network for audio-visual event localization and video parsing. In *Proceedings of the 30th ACM International Conference on Multimedia*. 6241–6249.
 - [51] Jing Zhang, Jianwen Xie, Nick Barnes, and Ping Li. 2021. Learning generative vision transformer with energy-based latent space for saliency prediction. *Advances in Neural Information Processing Systems* 34 (2021), 15448–15463.
 - [52] Yurong Zhang, Liulei Li, Wenguan Wang, Rong Xie, Li Song, and Wenjun Zhang. 2023. Boosting Video Object Segmentation via Space-time Correspondence Learning. In *Proceedings of the IEEE/CVF Conference on Computer Vision and Pattern Recognition*. 2246–2256.
 - [53] Sixiao Zheng, Jiachen Lu, Hengshuang Zhao, Xiatian Zhu, Zekun Luo, Yabiao Wang, Yanwei Fu, Jianfeng Feng, Tao Xiang, Philip H. S. Torr, and Li Zhang. 2021. Rethinking Semantic Segmentation From a Sequence-to-Sequence Perspective With Transformers. In *IEEE Conference on Computer Vision and Pattern Recognition, CVPR 2021, virtual, June 19-25, 2021*. Computer Vision Foundation / IEEE, 6881–6890. <https://doi.org/10.1109/CVPR46437.2021.00681>
 - [54] Jinxing Zhou, Xuyang Shen, Jianyuan Wang, Jiayi Zhang, Weixuan Sun, Jing Zhang, Stan Birchfield, Dan Guo, Lingpeng Kong, Meng Wang, et al. 2023. Audio-Visual Segmentation with Semantics. *arXiv preprint arXiv:2301.13190* (2023).
 - [55] Jinxing Zhou, Jianyuan Wang, Jiayi Zhang, Weixuan Sun, Jing Zhang, Stan Birchfield, Dan Guo, Lingpeng Kong, Meng Wang, and Yiran Zhong. 2022. Audio-Visual Segmentation. In *Computer Vision - ECCV 2022 - 17th European Conference, Tel Aviv, Israel, October 23-27, 2022, Proceedings, Part XXXVII (Lecture Notes in Computer Science, Vol. 13697)*, Shai Avidan, Gabriel J. Brostow, Moustapha Cissé, Giovanni Maria Farinella, and Tal Hassner (Eds.). Springer, 386–403. https://doi.org/10.1007/978-3-031-19836-6_22
 - [56] Jinxing Zhou, Liang Zheng, Yiran Zhong, Shijie Hao, and Meng Wang. 2021. Positive sample propagation along the audio-visual event line. In *Proceedings of the IEEE/CVF Conference on Computer Vision and Pattern Recognition*. 8436–8444.
 - [57] Xizhou Zhu, Weijie Su, Lewei Lu, Bin Li, Xiaogang Wang, and Jifeng Dai. 2021. Deformable DETR: Deformable Transformers for End-to-End Object Detection. In *9th International Conference on Learning Representations, ICLR 2021, Virtual Event, Austria, May 3-7, 2021*. OpenReview.net. <https://openreview.net/forum?id=gZ9hCDWe6ke>
 - [58] Xueyan Zou, Jianwei Yang, Hao Zhang, Feng Li, Linjie Li, Jianfeng Gao, and Yong Jae Lee. 2023. Segment everything everywhere all at once. *arXiv preprint arXiv:2304.06718* (2023).